AIMS Mathematics, 8(6): 14684–14703.
DOI: 10.3934/math.2023751
Received: 11 February 2023
Revised: 27 March 2023
Accepted: 30 March 2023
Published: 20 April 2023

http://www.aimspress.com/journal/Math

Research article

Delay-dependent anti-disturbance control of electric vehicle based on collective observers

Zigui Kang[1], **Tao Li**[2,*] **and Xiaofei Fan**[3]

[1] School of Electronics and Information Engineering, Nanjing University of Information Science and Technology, Nanjing, 210044, China
[2] Jiangsu Collaborative Innovation Center of Atmospheric Environment and Equipment Technology (CICAEET), Nanjing University of Information Science and Technology, Nanjing, 210044, China
[3] School of Automation, Nanjing University of Information Science and Technology, Nanjing, 210044, China

* **Correspondence:** Email: litaojia@163.com.

Abstract: An improved anti-disturbance strategy is proposed to guarantee lateral stability for electric vehicles with external disturbance and input time delay. Firstly, the T-S fuzzy model is applied to describe active front wheel steering system (AFS). Based on the obtained model, a new collective observers including disturbance observer and state observer are structured to estimate disturbance and state simultaneously. Then, a compound control is designed by using the estimation values of collective observers. During the design process, a novel path-independent fuzzy Lyapunov-Krasovskii function (FLKF) and slack variable matrices are introduced to reduce conservatism. Finally, two simulation cases are implemented on Matlab/Simulink-Carsim to show the effectiveness of the proposed method.

Keywords: vehicle lateral stability; collective observers; anti-disturbance control; input time-delay; path-independent FLKF

1. Introduction

With the development of electric vehicles, vehicle lateral stability based on AFS becomes more important. The vehicle lateral stability is the key performance to determining passenger safety and ride comfort [1–3]. This performance is mainly reflected in the vehicle lateral speed and yaw rate. The main factors affecting lateral stability are the side wind force, tire-road friction coefficient and the steering of the vehicle front wheels [4]. Specially, strong winds as the main disturbances will lead to lateral instability for AFS, so there have been many works on lateral stability control of vehicles in the presence of disturbances [5–8]. However, the above references do not make full use of disturbance

information in suppressing disturbance. There is still need to improve anti-disturbance capabilities for AFS. Disturbance observer based control (DOBC) is an effective rejection by using the estimated values of disturbances, which has been used successfully in robots, motor drives and missiles [9–19]. In [20], disturbance observer (DO) and H_∞ are used in flexible spacecraft with unknown disturbances. In [21], an active disturbance rejection sliding mode control based direct yaw-moment control system is presented. In [22], a composite controller by combining sliding mode control (SMC) and nonlinear disturbance observer (NDOB) is investigated. It is worth pointing out that the system states are known in [20–22]. However, the measurement of the vehicle lateral velocity requires expensive sensors, so it is necessary to study anti-disturbance control with unknown lateral velocity.

Considering the application of communication networks in vehicle control, it is inevitable that there exists time-delay during the signal transmissions and data dropout [23–25], which can lead to instability of the systems. Recently, some lateral stability control methods for vehicles with time delay have been studied. A delay dependent H_∞ control scheme is proposed to improve the vehicle stability and tracking performance of the AFS [23]. A robust sliding mode controller is designed to improve the lateral stability of vehicles with time delay [24]. To deal with the problem of multiple-package transmission and time varying delays for electric vehicles, a hybrid schedule-control scheme is developed including a new multiple-package transmission scheduler and an H_∞ control in [25]. However, the above studies do not take input time-delay into consideration. The input time delay from controller to actuator (CA) channel will bring negative effects on the closed-loop control system. To the best knowledge of authors, few results have been reported on anti-disturbance vehicle control based on observers with input time delay, which inspired our work.

T-S fuzzy algorithm is a very effective tool for nonlinear systems with uncertain parameters. Lots of fuzzy control schemes have been reported on vehicle lateral stability. For instance, a fuzzy observer based outputs feedback controller is designed for vehicle path tracking in [26]. A robust fuzzy control scheme is presented to enhance the vehicle lateral stability and handling performance [27]. A fuzzy observer-based event-triggered method control strategy is proposed for vehicle lane keeping capability and network bandwidth utilization [28]. However, the above researches are demonstrated by considering the common Lyapunov function (CLF), which may derive conservative results. The method based on fuzzy Lyapunov functions (FLF) can reduce conservatism. Some relative results are studied by using the time derivative of membership functions [29–33]. But when the membership functions are non-differentiable, these methods are not available. In [34], a path-independent fuzzy Lyapunov function (FLF) is proposed to reduce the conservatism, in which the time derivative of membership function (TDMF) is unknown. Note that the method in [34] does not take into account the time-delay case. In order to reduce the conservatism of the time-delayed system, a new path-independent fuzzy Lyapunov-Krasovskii function (FLKF) is proposed.

Therefore, this paper studies anti-disturbance control for AFS with input time-delay. The first step is to design collective observers to estimate the state and disturbance. The second step is to design the anti-disturbance controller to make closed-loop system stable. A new path-independent FLKF is constructed to reduce system conservatism. The main contributions of this paper are summarized below:

1) Compared with the results in [28, 35], anti-disturbance control is further considered by using collective observers. Meanwhile, this paper further extends the method in [22, 36] to the input time-delay case.

2) New collective observers are proposed to estimate the state and disturbance simultaneously. The collective observers include a disturbance observer and a state observer with information interaction.
3) A novel path-independent FLKF and slack variable matrices are used to reduce the design conservatism of collective observers and anti-disturbance controller. The proposed path-independent FLKF extends the path-independent FLF in [34] so that it can still be used in time-delayed systems.

The rest of this paper is organized as follows: system modeling, collective observers and anti-disturbance control structure are presented in Section 2. Section 3 presents main results of the collective observers, conservatism comparison and anti-disturbance controller. Section 4 illustrates two case simulations to verify the effectiveness of proposed control strategy. Finally, Section 5 concludes this paper.

2. System modeling and problem formulation

2.1. Vehicle dynamic model

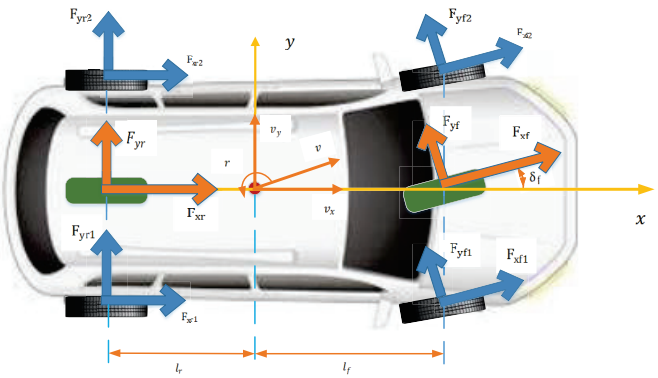

Figure 1. Vehicle lateral dynamics model.

In order to facilitate the system analysis, a two-degree-of-freedom (2-DOF) model is used to describe AFS (seen in Figure 1) [37]. And it has been verified that 2-DOF model is reasonable to describe dynamic performance of real driving vehicle when the tire-ground steering angle is small [6]. Taking into account the side wind force as the external disturbance, a vehicle AFS is modeled as:

$$\begin{cases} m_v(\dot{v}_y(t) + v_x r(t)) = F_{yf}(t) + F_{yr}(t) + F_w(t), \\ I_z\dot{r}(t) = l_f F_{yf}(t) - l_r F_{yr}(t) + l_f F_w(t), \end{cases} \tag{2.1}$$

where m_v is total mass of the vehicle, v_x and $v_y(t)$ are the vehicle longitudinal and lateral speed, respectively. $r(t)$ is the yaw rate. $F_{yf}(t)$ and $F_{yr}(t)$ are front and rear tire lateral forces. I_z denotes the yaw moment of inertia, l_f and l_r are the distance from the front and rear axles to the center of gravity. $F_w(t)$ is the side wind force. $\dot{F}_w(t)$ is the time derivative of side wind force, which will be used later in the design of the collective observers. $F_{yf}(t)$ and $F_{yr}(t)$ can be represented as:

$$F_{yf}(t) = C_f(\delta_f(t) - \frac{l_f r(t) + v_y(t)}{v_x}), \qquad F_{yr}(t) = C_r(\frac{l_r r(t) - v_y(t)}{v_x}), \tag{2.2}$$

where C_f and C_r are the front and rear tire cornering stiffness, respectively. And $\delta_f(t)$ is the front wheel angle.

An input time-delay is expressed as $\delta_f(t-\tau(t))$. By defining $x(t) = [v_y(t),\ r(t)]^T$ and $w(t) = \frac{1}{C_f}F_w(t)$, the following system can be obtained:

$$\begin{cases} \dot{x}(t) = Ax(t) + B(\delta_f(t-\tau(t)) + w(t)), \\ y(t) = Cx(t), \end{cases} \tag{2.3}$$

where

$$A = \begin{bmatrix} -\frac{C_f+C_r}{m_v v_x} & \frac{l_r C_r - l_f C_f}{m_v v_x} - v_x \\ \frac{l_r C_r - l_f C_f}{I_z v_x} & -\frac{{l_f}^2 C_f + {l_r}^2 C_r}{I_z v_x} \end{bmatrix}, \ B = \begin{bmatrix} \frac{C_f}{m_v} \\ \frac{l_f C_f}{I_z} \end{bmatrix}, \ C = \begin{bmatrix} 0 & 1 \end{bmatrix}.$$

$y(t)$ is the measurement output. $\tau(t)$ is the time-varying delay and satisfies $0 \le \tau(t) \le \tau_h$, τ_h is the maximum of the time delay.

Remark 1. Time varying-delay exists widely in in-vehicle networks control system [23–25], which is caused by signal transmission and data dropout. In practical, the upper limit of the delay requires a certain reliability of the system hardware, such as Controller Area Network (CAN) and FlexRay.

Remark 2. Since the payload and number of passengers may change, which changes the vehicle mass m_v and yaw moment of inertia I_z, thus m_v and I_z are considered as variables. This paper considers a situation that the vehicle longitudinal speed v_x is a fixed value [35]. In this case, the variables of the system can be confirmed as two variables m_v and I_z.

Remark 3. In this paper, the vehicle lateral velocity $v_y(t)$ is not measurable and the side wind force $F_w(t)$ is unknown. Thus, the state and disturbance observers are constructed simultaneously. Some works on disturbance observer assume that the disturbance is a constant [18, 38]. In practice, the side wind force $F_w(t)$ is time derivative. It is necessary to consider the case of time varying disturbance.

Define the maximum value and minimum value of vehicle mass as m_{max} and m_{min}, the maximum value and minimum value of vehicle yaw moment of inertia as I_{zmax} and I_{zmin}. $\iota_1 = \frac{1}{m_v}$, $\iota_2 = \frac{1}{I_z}$ and

$$\overline{m} = max\{\iota_1\} = \frac{1}{m_{min}}, \quad \underline{m} = min\{\iota_1\} = \frac{1}{m_{max}}, \quad \overline{I_z} = max\{\iota_2\} = \frac{1}{I_{zmin}}, \quad \underline{I_z} = min\{\iota_2\} = \frac{1}{I_{zmax}}. \tag{2.4}$$

The T-S fuzzy model is established to describe system (2.3), where the variables ι_1 and ι_2 are premise variables. Then, the membership functions can be obtained as follows.

$$\begin{cases} h_1(\iota) = M_1(\iota_1) \times N_1(\iota_2) \\ h_2(\iota) = M_2(\iota_1) \times N_1(\iota_2) \\ h_3(\iota) = M_1(\iota_1) \times N_2(\iota_2) \\ h_4(\iota) = M_2(\iota_1) \times N_2(\iota_2) \end{cases} \tag{2.5}$$

where $\iota = [\iota_1\ \iota_2]$, $h_i(\iota) \ge 0$, $\sum_{i=1}^{4} h_i(\iota) = 1$ and

$$\begin{cases} M_1(\iota_1) = \frac{\iota_1 - \underline{m}}{\overline{m} - \underline{m}}, \quad M_2(\iota_1) = \frac{\overline{m} - \iota_1}{\overline{m} - \underline{m}}. \\ N_1(\iota_2) = \frac{\iota_2 - \underline{I_z}}{\overline{I_z} - \underline{I_z}}, \quad N_2(\iota_2) = \frac{\overline{I_z} - \iota_2}{\overline{I_z} - \underline{I_z}}. \end{cases} \tag{2.6}$$

The T-S fuzzy model can be given to express nonlinear vehicle lateral dynamics as follows.

Model rule i: IF ι_1 is $M_{\mu 1}(\iota_1)$ and ι_2 is $N_{\mu 2}(\iota_2)$.

THEN

$$\begin{cases} \dot{x}(t) = A_i x(t) + B_i(\delta_f(t - \tau(t)) + w(t)), \\ y(t) = Cx(t), \end{cases} \tag{2.7}$$

where $\mu 1, \mu 2 = 1, 2$, $i = 1, 2, 3, 4$, the matrices A_i and B_i are given by replacing the parameters $1/m_v$ and $1/I_z$ in system (2.3) with $\overline{m}/(\underline{m})$ and $\overline{I_z}/(\underline{I_z})$.

Then, by the technique of defuzzification, the fuzzy subsystem (2.7) can be expressed in the following form:

$$\begin{cases} \dot{x}(t) = \sum_{i=1}^{4} h_i(\iota)[A_i x(t) + B_i(\delta_f(t - \tau(t)) + w(t))], \\ y(t) = Cx(t). \end{cases} \tag{2.8}$$

Remark 4. Note that the fuzzy premise variables m_v and I_z are non-differentiable, and it is clear that the derivative of membership functions can not be obtained. This characteristic causes a problem that traditional FLF can not be available in this case. By means of path-independent FLF [34], a new path-independent FLKF is developed to reduce conservatism for time delayed systems.

Remark 5. From [34], the path-independent FLF is given as: $V(x(t)) = x^T(t) \sum_{i=1}^{r} h_i(\iota)(P_0 + P_i)x(t)$ with $P_0 + P_i > 0$, $P_0 = P_0^T$ and $P_i = diag\{P_{11}^i, P_{22}^i, \cdots, P_{nn}^i\}$. It is noted that this method does not need the upper bound of the TDMF. Hence, the path-independent FLF eliminates the influence of TDMF.

In order to facilitate derivations in the main result, the following assumption and lemmas are given.

Assumption 1. Assume that the derivative of disturbance $w(t)$ satisfies: $\dot{w}(t) \in L_2[0, \infty)$.

Lemma 1 [35]. For known matrices X and Y with appropriate dimensions, the existence of any positive definite matrix Z makes the following inequality hold:

$$-2X^T Y \leq X^T Z^{-1} X + Y^T Z Y. \tag{2.9}$$

Lemma 2 [34]. For matrices U_{ij} with proper dimensions, the sufficient conditions of inequality $\sum_{i=1}^{r} \sum_{j=1}^{r} h_i(x) h_j(x) U_{ij} < 0$ is given as:

$$\begin{cases} U_{ii} < 0, \ i = 1, 2, \cdots, r. \\ \frac{1}{r-1} U_{ii} + \frac{1}{2}(U_{ij} + U_{ji}) < 0, \ i \neq j, \ i, j = 1, 2, \cdots, r. \end{cases} \tag{2.10}$$

2.2. Collective observers and anti-disturbance control structure

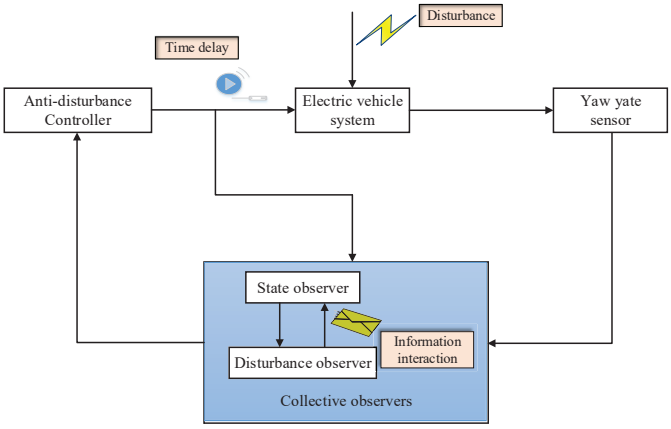

Figure 2. Anti-disturbance control structure.

The structure of the collective observers refers to the literature [20, 38, 39]. Figure 2 shows the proposed control scheme based on collective observers. In the collective observers structure, information interacts between state observer and disturbance observer. The fuzzy collective observers are structured based on (2.8) as:

$$\begin{cases} \dot{\hat{x}}(t) = \sum_{i=1}^{4}\sum_{j=1}^{4} h_i(\iota)h_j(\iota)[A_i\hat{x}(t) + B_i(\delta_f(t) + \hat{w}(t)) + L_{sj}(y(t) - C\hat{x}(t-\tau(t)))], \\ \dot{g}(t) = -\sum_{i=1}^{4}\sum_{j=1}^{4} h_i(\iota)h_j(\iota)L_{dj}C[A_i\hat{x}(t-\tau(t)) + B_i(\delta_f(t-\tau(t)) + \hat{w}(t-\tau(t)))], \\ \hat{w}(t) = \sum_{i=1}^{4}\sum_{j=1}^{4} h_i(\iota)h_j(\iota)[g(t) + L_{dj}y(t)], \end{cases} \tag{2.11}$$

where $\hat{x}(t)$ and $\hat{w}(t)$ are the estimation of state and disturbance, respectively. $g(t)$ stands for the auxiliary variable of the disturbance observer, L_{sj} and L_{dj} are the state observer gains and disturbance observer gains, respectively.

Remark 6. Unmeasurable state makes disturbance observer (DO) can not be formulated only by using the DO form as in [20]. In [38], disturbance observer and state observer are designed simultaneously but do not take into account the time-delay. Different from the design in [20, 38], the collective observers are used to estimate state and disturbance in the time-delay case.

Remark 7. The existence of input time delay $\tau(t)$ lead the disturbance $w(t)$ and states $x(t)$ only can be estimated at the time $t - \tau(t)$ [20]. The state estimation error and disturbance estimation error are defined as£ $e_x(t) = x(t) - \hat{x}(t-\tau(t))$, $e_w(t) = w(t) - \hat{w}(t-\tau(t))$. For constructing the standard error dynamics, the collective observers can be structured as in (2.11).

After constructing the collective observers, an anti-disturbance controller based on collective observers is proposed by referring [39].

$$\delta_f(t) = \sum_{i=1}^{4} h_i(\iota)[-\hat{w}(t) + K_i\hat{x}(t)]. \tag{2.12}$$

The estimation errors of collective observers are as follows:

$$\begin{cases} \dot{\varrho}(t) = \sum_{i=1}^{4}\sum_{j=1}^{4} h_i(\iota)h_j(\iota)[A_{\varrho i}\varrho(t) + B_{\varrho i j}\varrho(t-\tau(t)) + E_\varrho\dot{w}(t)], \\ z_\varrho(t) = C_\varrho\varrho(t), \end{cases} \tag{2.13}$$

where $z_\varrho(t)$ is the control output of the estimation errors system (2.13), $\varrho(t) = [e_x^T(t),\ e_w^T(t)]^T$, and

$$A_{\varrho i} = \begin{bmatrix} A_i & B_i \\ 0 & 0 \end{bmatrix},\ B_{\varrho i} = \begin{bmatrix} -L_{sj}C & 0 \\ -L_{dj}CA_i & -L_{dj}CB_i \end{bmatrix},\ E_\varrho = \begin{bmatrix} 0 \\ I \end{bmatrix},\ C_\varrho = \begin{bmatrix} 0 & I \end{bmatrix}.$$

Combining (2.8), (2.12) with (2.13), the closed loop control system is inferred as:

$$\begin{cases} \dot{\zeta}(t) = \sum_{i=1}^{4}\sum_{j=1}^{4} h_i(\iota)h_j(\iota)[A_{\zeta ij}\zeta(t) + B_{\zeta ij}\zeta(t-\tau(t)) + E_\zeta\dot{w}(t)], \\ z_\zeta(t) = C_\zeta\zeta(t), \end{cases} \tag{2.14}$$

where $z_\zeta(t)$ is the control output of the closed loop control system (2.14), $\zeta(t) = [x^T(t),\ e_x^T(t),\ e_w^T(t)]^T$, and

$$A_{\zeta ij} = \begin{bmatrix} A_i + B_iK_j & -B_iK_j & B_i \\ 0 & A_i & B_i \\ 0 & 0 & 0 \end{bmatrix},\ B_{\zeta i} = \begin{bmatrix} 0 & 0 & 0 \\ 0 & -L_{sj}C & 0 \\ 0 & -L_{dj}CA_i & -L_{dj}CB_i \end{bmatrix},\ E_\zeta = \begin{bmatrix} 0 \\ 0 \\ I \end{bmatrix},\ C_\zeta = \begin{bmatrix} I & 0 & 0 \end{bmatrix}.$$

The estimation error system (2.13) is asymptotically stable and satisfies the H_∞ performance with γ_1 attenuation level, when the following conditions are satisfied as:

$$\int_0^\infty z_\varrho{}^T(t) z_\varrho(t) dt < \gamma_1{}^2 \int_0^\infty \dot{w}^T(t) \dot{w}(t) dt. \tag{2.15}$$

3. Main results

3.1. Collective observers design

To obtain the feasible observer gains in (2.11), we need to analyze the stability of the estimation error system (2.13). Then, the following theorem is given.

Theorem 1. The estimation error system (2.13) is asymptotically stable if there exist symmetric matrices $P_{\varrho 0}$, $Q_{\varrho 0}$, $R_{\varrho 0}$, diagonal matrices $P_{\varrho i}$, $Q_{\varrho i}$, $R_{\varrho i}$, arbitrary matrix M_ϱ, Z_{si}, Z_{di}, given scalar $\gamma_1 > 0$ and λ_1 satisfying the following inequalities:

$$\begin{cases} \Xi_{ii} < 0, \\ \frac{1}{3}\Xi_{ii} + \frac{1}{2}(\Xi_{ij} + \Xi_{ji}) < 0, \ i \neq j, \end{cases} \tag{3.1}$$

$$P_{\varrho 0} + P_{\varrho i} > 0, \quad Q_{\varrho 0} + Q_{\varrho i} > 0, \quad R_{\varrho 0} + R_{\varrho i} > 0. \tag{3.2}$$

where i=1,2,3,4.

$$\Xi_{ij} = \begin{bmatrix} \theta_{11}^i & \theta_{12}^{ij} & 0 & 0 & 0 \\ * & \theta_{22}^i & 0 & \theta_{24} & \theta_{25}^{ij} \\ * & * & \theta_{33}^i & 0 & 0 \\ * & * & * & -\gamma_1{}^2 I & 0 \\ * & * & * & * & \theta_{55}^i \end{bmatrix},$$

$$\theta_{11}^i = Q_{\varrho 0} + Q_{\varrho i} - \tfrac{2}{\lambda_1}(P_{\varrho 0} + P_{\varrho i}) + \tfrac{\tau_h}{\lambda_1{}^2}(R_{\varrho 0} + R_{\varrho i}) + C_\varrho{}^T C_\varrho,$$

$$\theta_{12}^{ij} = P_{\varrho 0} + P_{\varrho i} + M_\varrho + \lambda_1 (A_{\varrho i} + B_{\varrho ij})^T M_\varrho - \tfrac{\tau_h}{\lambda_1}(R_{\varrho 0} + R_{\varrho i}), \qquad \theta_{22}^i = -\lambda_1 M_\varrho - \lambda_1 M_\varrho{}^T + \tau_h (R_{\varrho 0} + R_{\varrho i}),$$

$$\theta_{24} = \lambda_1 M_\varrho{}^T E_\varrho, \qquad \theta_{25}^{ij} = \lambda_1 M_\varrho{}^T B_{\varrho ij}, \qquad \theta_{33}^i = -Q_{\varrho 0} - Q_{\varrho i}, \qquad \theta_{55}^i = -\tau_h^{-1}(R_{\varrho 0} + R_{\varrho i}),$$

$$P_{\varrho 0} = \begin{bmatrix} P_{\varrho 0}^{11} & P_{\varrho 0}^{12} \\ * & P_{\varrho 0}^{22} \end{bmatrix}, \quad Q_{\varrho 0} = \begin{bmatrix} Q_{\varrho 0}^{11} & Q_{\varrho 0}^{12} \\ * & Q_{\varrho 0}^{22} \end{bmatrix}, \quad R_{\varrho 0} = \begin{bmatrix} R_{\varrho 0}^{11} & R_{\varrho 0}^{12} \\ * & R_{\varrho 0}^{22} \end{bmatrix}, \quad P_{\varrho i} = \begin{bmatrix} P_{\varrho i}^{11} & 0 \\ * & P_{\varrho i}^{22} \end{bmatrix},$$

$$Q_{\varrho i} = \begin{bmatrix} Q_{\varrho i}^{11} & 0 \\ * & Q_{\varrho i}^{22} \end{bmatrix}, \quad R_{\varrho i} = \begin{bmatrix} R_{\varrho i}^{11} & 0 \\ * & R_{\varrho i}^{22} \end{bmatrix}, \quad M_\varrho = \begin{bmatrix} M_{\varrho 1} & 0 \\ 0 & M_{\varrho 2} \end{bmatrix},$$

$$A_{\varrho i}{}^T M_\varrho = \begin{bmatrix} A_i{}^T M_{\varrho 1} & 0 \\ B_i{}^T M_{\varrho 1} & 0 \end{bmatrix}, \quad B_{\varrho ij}{}^T M_\varrho = \begin{bmatrix} -C^T Z_{sj}{}^T & -A_i{}^T C^T Z_{dj}{}^T \\ 0 & -B_i{}^T C^T Z_{dj}{}^T \end{bmatrix}.$$

then, the observer gains are obtained as $L_{sj} = M_{\varrho 1}{}^{T^{-1}} Z_{sj}$ and $L_{dj} = M_{\varrho 2}{}^{T^{-1}} Z_{dj}$.

Proof. By using Newton-Leibniz formula [35] as:

$$\varrho(t - \tau(t)) = \varrho(t) - \int_{t-\tau(t)}^{t} \dot{\varrho}(s) ds. \tag{3.3}$$

The estimation error system (2.13) is transformed into:

$$\dot{\varrho}(t) = \sum_{i=1}^{4}\sum_{j=1}^{4} h_i(\iota)h_j(\iota)\left[(A_{\varrho i} + B_{\varrho ij})\varrho(t) - B_{\varrho ij}\int_{t-\tau(t)}^{t}\dot{\varrho}(s)ds + E_{\varrho}\dot{w}(t)\right]. \tag{3.4}$$

The system (3.4) can be rewritten as a description system as follow:

$$\bar{E}_{\varrho}\dot{\varepsilon}_{\varrho}(t) = \sum_{i=1}^{4}\sum_{j=1}^{4} h_i(\iota)h_j(\iota)\left[\bar{A}_{\varrho ij}\varepsilon_{\varrho}(t) - \bar{B}_{\varrho ij}\int_{t-\tau(t)}^{t}\dot{\varrho}(s)ds + \bar{E}_{\varrho}\dot{w}(t)\right], \tag{3.5}$$

where $\bar{E}_{\varrho} = \begin{bmatrix} I & 0 \\ 0 & 0 \end{bmatrix}$, $\bar{A}_{\varrho ij} = \begin{bmatrix} 0 & I \\ A_{\varrho i} + B_{\varrho ij} & -I \end{bmatrix}$, $\bar{B}_{\varrho ij} = \begin{bmatrix} 0 \\ B_{\varrho ij} \end{bmatrix}$, $\bar{E}_{\varrho} = \begin{bmatrix} 0 \\ E_{\varrho} \end{bmatrix}$, $\varepsilon_{\varrho}(t) = \begin{bmatrix} \varrho(t) \\ \dot{\varrho}(t) \end{bmatrix}$.

As stated in Remark 4, the membership functions are non-differentiable. A new path-independent FLKF is constructed to reduce conservatism as:

$$V(\varrho(t)) = \varrho^T(t)P_{\varrho}(\iota)\varrho(t) + \int_{t-\tau_h}^{t}\varrho^T(s)Q_{\varrho}(\iota)\varrho(s)ds + \int_{-\tau_h}^{0}\int_{t+\theta}^{t}\dot{\varrho}^T(s)R_{\varrho}(\iota)\dot{\varrho}(s)dsd\theta, \tag{3.6}$$

where $P_{\varrho}(\iota) = \sum_{i=1}^{4} h_i(\iota)(P_{\varrho 0} + P_{\varrho i})$, $Q_{\varrho}(\iota) = \sum_{i=1}^{4} h_i(\iota)(Q_{\varrho 0} + Q_{\varrho i})$, $R_{\varrho}(\iota) = \sum_{i=1}^{4} h_i(\iota)(R_{\varrho 0} + R_{\varrho i})$.

For simplify the writing, define $\sum_{i=1}^{4} h_i(\iota)A_{\varrho i} = A_{\varrho h}$ and $\sum_{i=1}^{4}\sum_{j=1}^{4} h_i(\iota)h_j(\iota)B_{\varrho ij} = B_{\varrho h}$. To decouple $P_{\varrho}(\iota)$ from system matrix $A_{\varrho h}$, slack variables M_{ϱ} and $\lambda_1 M_{\varrho}$ are introduced as follows [34].

$$\begin{aligned}
\dot{V}(\varrho(t)) = {} & 2\begin{bmatrix} \varrho(t) \\ \dot{\varrho}(t) \end{bmatrix}^T \begin{bmatrix} P_{\varrho}(\iota) & 0 \\ M_{\varrho} & \lambda_1 M_{\varrho} \end{bmatrix}\begin{bmatrix} \dot{\varrho}(t) \\ S_{\varrho} \end{bmatrix} + \varrho^T(t)Q_{\varrho}(\iota)\varrho(t) - \varrho^T(t-\tau_h)Q_{\varrho}(\iota)\varrho(t-\tau_h) + \\
& \tau_h\dot{\varrho}^T(t)R_{\varrho}(\iota)\dot{\varrho}(t) - \int_{t-\tau_h}^{t}\dot{\varrho}^T(s)R_{\varrho}(\iota)\dot{\varrho}(s)ds \\
\leq {} & \begin{bmatrix} \varrho(t) \\ \dot{\varrho}(t) \end{bmatrix}^T \begin{bmatrix} \Theta_{\rho}^{11} & \Theta_{\rho}^{12} \\ * & \Theta_{\rho}^{22} \end{bmatrix}\begin{bmatrix} \varrho(t) \\ \dot{\varrho}(t) \end{bmatrix} - 2\begin{bmatrix} \varrho(t) \\ \dot{\varrho}(t) \end{bmatrix}^T \begin{bmatrix} M_{\varrho}{}^T B_{\varrho h} \\ \lambda_1 M_{\varrho}{}^T B_{\varrho h} \end{bmatrix}\int_{t-\tau(t)}^{t}\dot{\varrho}(s)ds + 2\begin{bmatrix} \varrho(t) \\ \dot{\varrho}(t) \end{bmatrix}^T \\
& \begin{bmatrix} M_{\varrho}{}^T E_{\varrho} \\ \lambda_1 M_{\varrho}{}^T E_{\varrho} \end{bmatrix}\dot{w}(t) + \varrho^T(t)Q_{\varrho}(\iota)\varrho(t) - \varrho^T(t-\tau_h)Q_{\varrho}(\iota)\varrho(t-\tau_h) + \tau_h\dot{\varrho}^T(t)R_{\varrho}(\iota)\dot{\varrho}(t) - \\
& \int_{t-\tau_h}^{t}\dot{\varrho}^T(s)R_{\varrho}(\iota)\dot{\varrho}(s)ds,
\end{aligned} \tag{3.7}$$

where

$S_{\varrho} = (A_{\varrho h} + B_{\varrho h})\varrho(t) - B_{\varrho h}\int_{t-\tau(t)}^{t}\dot{\varrho}(s)ds + E_{\varrho}\dot{w}(t)$, $\Theta_{\varrho}^{11} = M_{\varrho}{}^T(A_{\varrho h} + B_{\varrho h}) + (A_{\varrho h} + B_{\varrho h})^T M_{\varrho}$,

$\Theta_{\varrho}^{12} = P_{\varrho}(\iota) - M_{\varrho}{}^T + \lambda_1(A_{\varrho h} + B_{\varrho h})^T M_{\varrho}$, $\Theta_{\varrho}^{22} = -\lambda_1 M_{\varrho} - \lambda_1 M_{\varrho}{}^T$.

According to Lemma 1, the following inequality is hold:

$$\begin{aligned}
-2\begin{bmatrix} \varrho(t) \\ \dot{\varrho}(t) \end{bmatrix}^T \begin{bmatrix} M_{\varrho}{}^T B_{\varrho h} \\ \lambda_1 M_{\varrho}{}^T B_{\varrho h} \end{bmatrix}\int_{t-\tau(t)}^{t}\dot{\varrho}(s)ds \leq {} & \int_{t-\tau_h}^{t}\dot{\varrho}^T(s)R_{\varrho}(\iota)\dot{\varrho}(s)ds + \tau_h\begin{bmatrix} \varrho(t) \\ \dot{\varrho}(t) \end{bmatrix}^T \begin{bmatrix} M_{\varrho}{}^T B_{\varrho h} \\ \lambda_1 M_{\varrho}{}^T B_{\varrho h} \end{bmatrix}R_{\varrho}(\iota)^{-1} \\
& \begin{bmatrix} B_{\varrho h}^T M_{\varrho} & \lambda_1 B_{\varrho h}^T M_{\varrho} \end{bmatrix}\begin{bmatrix} \varrho(t) \\ \dot{\varrho}(t) \end{bmatrix},
\end{aligned} \tag{3.8}$$

Based on (2.15), (3.7) and (3.8), we have:

$$\dot{V}(\varrho(t)) + z_{\varrho}{}^T(t)z_{\varrho}(t) - \gamma_1{}^2\dot{w}^T(t)\dot{w}(t) \leq \begin{bmatrix} \varrho(t) \\ \dot{\varrho}(t) \\ \varrho(t-\tau_h) \\ \dot{w}(t) \end{bmatrix}^T \begin{bmatrix} \Upsilon_{\varrho}^{11} & \Upsilon_{\varrho}^{12} & 0 & \Upsilon_{\varrho}^{14} \\ * & \Upsilon_{\varrho}^{22} & 0 & \lambda_1\Upsilon_{\varrho}^{14} \\ * & * & \Upsilon_{\varrho}^{33} & 0 \\ * & * & * & -\gamma_1{}^2 \end{bmatrix}\begin{bmatrix} \varrho(t) \\ \dot{\varrho}(t) \\ \varrho(t-\tau_h) \\ \dot{w}(t) \end{bmatrix} < 0, \tag{3.9}$$

where
$\Upsilon_{\varrho}^{11} = M_{\varrho}{}^{T}(A_{\varrho h} + B_{\varrho h}) + (A_{\varrho h} + B_{\varrho h})^{T} M_{\varrho} + Q_{\varrho}(\iota) + \tau_h M_{\varrho}{}^{T} B_{\varrho h} R_{\varrho}^{-1}(\iota) B_{\varrho h}{}^{T} M_{\varrho} + C_{\varrho}{}^{T} C_{\varrho}$,
$\Upsilon_{\varrho}^{12} = P_{\varrho}(\iota) - M_{\varrho}{}^{T} + \lambda_1 (A_{\varrho h} + B_{\varrho h})^{T} M_{\varrho} + \tau_h \lambda_1 M_{\varrho}{}^{T} B_{\varrho h} R_{\varrho}^{-1}(\iota) B_{\varrho h}{}^{T} M_{\varrho}, \quad \Upsilon_{\varrho}^{14} = M_{\varrho}{}^{T} E_{\varrho}$,
$\Upsilon_{\varrho}^{22} = -\lambda_1 M_{\varrho}{}^{T} - \lambda_1 M_{\varrho} + \tau_h R_{\varrho}(\iota) + \tau_h \lambda_1^2 M_{\varrho}{}^{T} B_{\varrho h} R_{\varrho}^{-1}(\iota) B_{\varrho h}{}^{T} M_{\varrho}, \quad \Upsilon_{\varrho}^{33} = -Q_{\varrho}(\iota)$.

According to (3.9), the following matrix inequality can be inferred by using Schur complement:

$$\begin{bmatrix} \bar{\Upsilon}_{\varrho}^{11} & \bar{\Upsilon}_{\varrho}^{12} & 0 & \Upsilon_{\varrho}^{14} & \Upsilon_{\varrho}^{15} \\ * & \bar{\Upsilon}_{\varrho}^{22} & 0 & \lambda_1 \Upsilon_{\varrho}^{14} & \lambda_1 \Upsilon_{\varrho}^{15} \\ * & * & \Upsilon_{\varrho}^{33} & 0 & 0 \\ * & * & * & -{\gamma_1}^2 I & 0 \\ * & * & * & * & \Upsilon_{\varrho}^{55} \end{bmatrix} < 0, \tag{3.10}$$

where
$\bar{\Upsilon}_{\varrho}^{11} = M_{\varrho}{}^{T}(A_{\varrho h} + B_{\varrho h}) + (A_{\varrho h} + B_{\varrho h})^{T} M_{\varrho} + Q_{\varrho}(\iota) + C_{\varrho}{}^{T} C_{\varrho}, \quad \bar{\Upsilon}_{\varrho}^{12} = P_{\varrho}(\iota) - M_{\varrho}{}^{T} + \lambda_1 (A_{\varrho h} + B_{\varrho h})^{T} M_{\varrho}$,
$\bar{\Upsilon}_{\varrho}^{22} = -\lambda_1 M_{\varrho}{}^{T} - \lambda_1 M_{\varrho} + \tau_h R_{\varrho}(\iota), \quad \Upsilon_{\varrho}^{15} = M_{\varrho}{}^{T} B_{\varrho h}, \quad \Upsilon_{\varrho}^{55} = -{\tau_h}^{-1} R_{\varrho}(\iota)$.

Based on Lemma 2, the inequalities (3.1) can be obtained by pre-multiplying and post-multiplying by T_{ϱ} and $T_{\varrho}{}^{T}$ to (2.10), where

$$T_{\varrho} = \begin{bmatrix} I & -\frac{1}{\lambda_1} I & 0 & 0 & 0 \\ 0 & I & 0 & 0 & 0 \\ 0 & 0 & I & 0 & 0 \\ 0 & 0 & 0 & I & 0 \\ 0 & 0 & 0 & 0 & I \end{bmatrix}.$$

The proof is completed.

Remark 8. Discontinuous variables exist widely in practice, which leads to the unknowability of the derivative information of the membership function. The new path-independent FLKF provides a more relaxed approach for nonlinear time delay systems with discontinuous variables. This method extends the path-independent FLF in [34] to the analysis of time-delay systems, not only reducing the conservatism of the time-delay systems but also overcoming the limitations that TDMF must know.

Remark 9. The decoupling method used in (3.7) can reduce the number of variable cross-terms. This scheme can reduce computational complexity and help to find better optimal solutions. Different form fuzzy observer designed in [34], the slack variable matrices M_{ϱ} and $\lambda_1 M_{\varrho}$ are introduced in Theorem 1, where the added parameter λ_1 may improve freedom of observer gain. This method is also used in the design of the following anti-disturbance controller.

3.2. Conservatism comparison

To demonstrate the advantages of the novel path-independent FLKF and the slack variable matrices M_{ϱ} and $\lambda_1 M_{\varrho}$, Corollary 1 is given.

The estimation errors system (2.13) also can use the common Lyapunov-Krasovskii function (CLKF) [35]: $V(\varrho(t)) = \varrho^{T}(t) P \varrho(t) + \int_{t-\tau_h}^{t} \varrho^{T}(s) Q \varrho(s) ds + \int_{-\tau_h}^{0} \int_{t+\theta}^{t} \dot{\varrho}^{T}(s) R \dot{\varrho}(s) ds d\theta$ and introduced M_{ϱ} and $\lambda_1 M_{\varrho}$, the following corollary can be drawn.

Corollary 1. The estimation error system (2.13) is asymptotically stable when symmetric matrices P, Q, R, arbitrary matrix M_{ϱ}, Z_{si}, Z_{di}, given scalar $\gamma_1 > 0$ and λ_1 meet the following conditions:

$$\begin{cases} \Psi_{ii} < 0, \\ \frac{1}{3}\Psi_{ii} + \frac{1}{2}(\Psi_{ij} + \Psi_{ji}) < 0, \ i \neq j, \end{cases} \tag{3.11}$$

$$P > 0, \qquad Q > 0, \qquad R > 0. \tag{3.12}$$

where i=1,2,3,4.

$$\Psi_{ij} = \begin{bmatrix} \varpi_{11} & \varpi_{12}^{ij} & 0 & 0 & 0 \\ * & \varpi_{22} & 0 & \varpi_{24} & \varpi_{25}^{ij} \\ * & * & -Q & 0 & 0 \\ * & * & * & -{\gamma_1}^2 I & 0 \\ * & * & * & * & -\tau_h^{-1} R \end{bmatrix},$$

$\varpi_{11} = Q - \frac{2}{\lambda_1} P + \frac{\tau_h}{{\lambda_1}^2} R + {C_\varrho}^T C_\varrho$, $\varpi_{12}^{ij} = P + M_\varrho + \lambda_1 (A_{\varrho i} + B_{\varrho ij})^T M_\varrho - \frac{\tau_h}{\lambda_1} R$, $\varpi_{22} = -\lambda_1 M_\varrho - \lambda_1 {M_\varrho}^T + \tau_h R$, $\varpi_{24} = \lambda_1 {M_\varrho}^T E_\varrho$, $\varpi_{25}^{ij} = \lambda_1 {M_\varrho}^T B_{\varrho ij}$,

$$P = \begin{bmatrix} P_{11} & P_{12} \\ * & P_{22} \end{bmatrix}, \quad Q = \begin{bmatrix} Q_{11} & Q_{12} \\ * & Q_{22} \end{bmatrix}, \quad R = \begin{bmatrix} R_{11} & R_{12} \\ * & R_{22} \end{bmatrix}, \quad M_\varrho = \begin{bmatrix} M_{\varrho 1} & 0 \\ 0 & M_{\varrho 2} \end{bmatrix},$$

$$ {A_{\varrho i}}^T M_\varrho = \begin{bmatrix} {A_i}^T M_{\varrho 1} & 0 \\ {B_i}^T M_{\varrho 1} & 0 \end{bmatrix}, \quad {B_{\varrho ij}}^T M_\varrho = \begin{bmatrix} -C^T {Z_{sj}}^T & -{A_i}^T C^T {Z_{dj}}^T \\ 0 & -{B_i}^T C^T {Z_{dj}}^T \end{bmatrix}.$$

Remark 10. In [35], CLFK is used to analyze closed-loop state feedback control systems. However, for the analysis of collective estimation errors system (2.13), it is necessary to decouple variable matrix P from system matrices. Then, the looser variable matrices M_ϱ and $\lambda_1 M_\varrho$ are used in Corollary 1. Moreover, it is noted that the CLKF [35] is a special case of path-independent FLKF (3.6) by setting $P_{\varrho i} = 0$, $Q_{\varrho i} = 0$ and $R_{\varrho i} = 0$ in (3.1) and (3.2). Then, the inequalities (3.1) and (3.2) equivalent to inequalities (3.11) and (3.12). Thus, Theorem 1 has less conservative than Corollary 1.

Remark 11. λ_1 is a tunable parameter. Additionally, for the accuracy of the estimation of states and disturbance, a optimization method is given as: *min* γ_1 subject to (3.1) and (3.11). Similar to observer design, the following anti-disturbance controller design is also used *min* γ_2 subject to (3.13).

Remark 12. Because the decoupling method is used in the analysis produce, the path-independent FLKF proposed in this paper does not increase the computational complexity compared to CLKF [35]. While, the control strategy based on collective observers increases the step of the observer gains calculation compared with state feedback control based on H_∞.

3.3. Anti-disturbance controller design

Based on the observer gains, this part is to solve the anti-disturbance controller gains by analyzing the stability of closed loop control system (2.14). The result is given as follow.

Theorem 2. If there exist a positive given scalar γ_2, a given scalar λ_2, symmetric matrices $\hat{P}_{\zeta 0}$, $\hat{Q}_{\zeta 0}$, $\hat{R}_{\zeta 0}$, diagonal matrices $\hat{P}_{\zeta i}$, $\hat{Q}_{\zeta i}$, $\hat{R}_{\zeta i}$, arbitrary matrix $\hat{M}_\zeta$ and Z_{gi}. The closed loop control system (2.14) is asymptotically stable with H_∞ performance lever γ_2.

$$\begin{cases} \Pi_{ii} < 0, \\ \frac{1}{3}\Pi_{ii} + \frac{1}{2}(\Pi_{ij} + \Pi_{ji}) < 0, \ i \neq j. \end{cases} \tag{3.13}$$

$$\hat{P}_{\zeta 0} + \hat{P}_{\zeta i} > 0, \quad \hat{Q}_{\zeta 0} + \hat{Q}_{\zeta i} > 0, \quad \hat{R}_{\zeta 0} + \hat{R}_{\zeta i} > 0, \tag{3.14}$$

where i,j=1,2,3,4.

$$\Pi_{ij}=\begin{bmatrix} \hat{\psi}_{11}^{i} & \hat{\psi}_{12}^{ij} & 0 & 0 & 0 & \hat{M}_{\zeta}^{T} \\ * & \hat{\psi}_{22}^{i} & 0 & \hat{\psi}_{24} & \hat{\psi}_{25}^{ij} & 0 \\ * & * & \hat{\psi}_{33}^{i} & 0 & 0 & 0 \\ * & * & * & -{\gamma_1}^2 I & 0 & 0 \\ * & * & * & * & \hat{\psi}_{55}^{i} & 0 \\ * & * & * & * & * & -I \end{bmatrix},$$

$\hat{\psi}_{11}^{i}=\hat{Q}_{\zeta 0}+\hat{Q}_{\zeta i}-\frac{2}{\lambda_2}(\hat{P}_{\zeta 0}+\hat{P}_{\zeta i})+\frac{\tau_h}{{\lambda_2}^2}(\hat{R}_{\zeta 0}+\hat{R}_{\zeta i})$,
$\hat{\psi}_{12}^{ij}=\hat{P}_{\zeta 0}+\hat{P}_{\zeta i}+\hat{M}_{\zeta}^{T}+\lambda_2\hat{M}_{\zeta}^{T}(A_{\zeta ij}+B_{\zeta ij})^{T}-\frac{\tau_h}{\lambda_2}(\hat{R}_{\zeta 0}+\hat{R}_{\zeta i})$, $\hat{\psi}_{22}^{i}=-\lambda_2\hat{M}_{\zeta}-\lambda_2\hat{M}_{\zeta}^{T}+\tau_h(\hat{R}_{\zeta 0}+\hat{R}_{\zeta i})$,
$\hat{\psi}_{24}=\lambda_2 E_{\zeta}$, $\hat{\psi}_{25}^{ij}=\lambda_2 B_{\zeta ij}\hat{M}_{\zeta}$£ $\hat{\psi}_{33}^{i}=-\hat{Q}_{\zeta 0}-\hat{Q}_{\zeta i}$, $\hat{\psi}_{55}^{i}=-\tau_h^{-1}(\hat{R}_{\zeta 0}+\hat{R}_{\zeta i})$,

$$\hat{P}_{\zeta 0}=\begin{bmatrix} \hat{P}_{\zeta 0}^{11} & \hat{P}_{\zeta 0}^{12} & \hat{P}_{\zeta 0}^{13} \\ * & \hat{P}_{\zeta 0}^{22} & \hat{P}_{\zeta 0}^{23} \\ * & * & \hat{P}_{\zeta 0}^{33} \end{bmatrix},\ \hat{Q}_{\zeta 0}=\begin{bmatrix} \hat{Q}_{\zeta 0}^{11} & \hat{Q}_{\zeta 0}^{12} & \hat{Q}_{\zeta 0}^{13} \\ * & \hat{Q}_{\zeta 0}^{22} & \hat{Q}_{\zeta 0}^{23} \\ * & * & \hat{Q}_{\zeta 0}^{33} \end{bmatrix},\ \hat{R}_{\zeta 0}=\begin{bmatrix} \hat{R}_{\zeta 0}^{11} & \hat{R}_{\zeta 0}^{12} & \hat{R}_{\zeta 0}^{13} \\ * & \hat{R}_{\zeta 0}^{22} & \hat{R}_{\zeta 0}^{23} \\ * & * & \hat{R}_{\zeta 0}^{33} \end{bmatrix},\ \hat{P}_{\zeta i}=\begin{bmatrix} \hat{P}_{\zeta i}^{11} & 0 & 0 \\ * & \hat{P}_{\zeta i}^{22} & 0 \\ * & * & \hat{P}_{\zeta i}^{33} \end{bmatrix},$$

$$\hat{Q}_{\zeta i}=\begin{bmatrix} \hat{Q}_{\zeta i}^{11} & 0 & 0 \\ * & \hat{Q}_{\zeta i}^{22} & 0 \\ * & * & \hat{Q}_{\zeta i}^{33} \end{bmatrix},\quad \hat{R}_{\zeta i}=\begin{bmatrix} \hat{R}_{\zeta i}^{11} & 0 & 0 \\ * & \hat{R}_{\zeta i}^{22} & 0 \\ * & * & \hat{R}_{\zeta i}^{33} \end{bmatrix},\quad \hat{M}_{\zeta}=\begin{bmatrix} \hat{M}_{\zeta 1} & 0 & 0 \\ 0 & \hat{M}_{\zeta 1} & 0 \\ 0 & 0 & \hat{M}_{\zeta 2} \end{bmatrix}.$$

$$\hat{M}_{\zeta}^{T}{A_{\zeta ij}}^{T}=\begin{bmatrix} \hat{M}_{\zeta 1}^{T}{A_i}^{T}+{Z_{gj}}^{T}{B_i}^{T} & 0 & 0 \\ -Z_{gj}^{T}{B_i}^{T} & \hat{M}_{\zeta 1}^{T}{A_i}^{T} & 0 \\ \hat{M}_{\zeta 2}^{T}{B_i}^{T} & \hat{M}_{\zeta 2}^{T}{B_i}^{T} & 0 \end{bmatrix},\quad \hat{M}_{\zeta}^{T}B_{\zeta ij}{}^{T}=\begin{bmatrix} 0 & 0 & 0 \\ 0 & -\hat{M}_{\zeta 1}^{T}C^{T}{L_{sj}}^{T} & -\hat{M}_{\zeta 1}^{T}{A_i}^{T}C^{T}{L_{dj}}^{T} \\ 0 & 0 & -\hat{M}_{\zeta 2}^{T}{B_i}^{T}C^{T}{L_{dj}}^{T} \end{bmatrix}.$$

Then, the anti-disturbance gains are $K_j=Z_{gj}\hat{M}_{\zeta 1}^{-1}$.

Proof. Choose the same path-independent FLKF as (3.6):

$$V(\zeta(t))=\zeta^{T}(t)P_{\zeta}(\iota)\zeta(t)+\int_{t-\tau_h}^{t}\zeta^{T}(s)Q_{\zeta}(\iota)\zeta(s)ds+\int_{-\tau_h}^{0}\int_{t+\theta}^{t}\dot{\zeta}^{T}(s)R_{\zeta}(\iota)\dot{\zeta}(s)dsd\theta. \tag{3.15}$$

Similar to (3.7) and (3.8), and by using (2.15), one has:

$$\begin{aligned} &\dot{V}(\zeta(t))+{z_{\zeta}}^{T}(t)z_{\zeta}(t)-{\gamma_2}^2\dot{w}^{T}(t)\dot{w}(t) \\ &\leq\begin{bmatrix} \zeta(t) \\ \dot{\zeta}(t) \\ \zeta(t-\tau_h) \\ \dot{w}(t) \end{bmatrix}^{T}\begin{bmatrix} \Upsilon_{\zeta}^{11} & \Upsilon_{\zeta}^{12} & 0 & \Upsilon_{\zeta}^{14} \\ * & \Upsilon_{\zeta}^{22} & 0 & \lambda_1\Upsilon_{\zeta}^{14} \\ * & * & \Upsilon_{\zeta}^{33} & 0 \\ * & * & * & -{\gamma_2}^2 \end{bmatrix}\begin{bmatrix} \zeta(t) \\ \dot{\zeta}(t) \\ \zeta(t-\tau_h) \\ \dot{w}(t) \end{bmatrix}<0. \end{aligned} \tag{3.16}$$

$\Upsilon_{\zeta}^{11}={M_{\zeta}}^{T}(A_{\zeta h}+B_{\zeta h})+(A_{\zeta h}+B_{\zeta h})^{T}M_{\zeta}+Q_{\zeta}(\iota)+\tau_h{M_{\zeta}}^{T}B_{\zeta h}R_{\zeta}^{-1}(\iota){B_{\zeta h}}^{T}M_{\zeta}+{C_{\zeta}}^{T}C_{\zeta}$,
$\Upsilon_{\zeta}^{12}=P_{\zeta}(\iota)-{M_{\zeta}}^{T}+\lambda_1(A_{\zeta h}+B_{\zeta h})^{T}M_{\zeta}+\tau_h\lambda_1{M_{\zeta}}^{T}B_{\zeta h}R_{\zeta}^{-1}(\iota){B_{\zeta h}}^{T}M_{\zeta}$, $\Upsilon_{\zeta}^{14}={M_{\zeta}}^{T}E_{\zeta}$
$\Upsilon_{\zeta}^{22}=-\lambda_1{M_{\zeta}}^{T}-\lambda_1M_{\zeta}+\tau_hR_{\zeta}(\iota)+\tau_h\lambda_1^2{M_{\zeta}}^{T}B_{\zeta h}R_{\zeta}^{-1}(\iota){B_{\zeta h}}^{T}M_{\zeta}$, $\Upsilon_{\zeta}^{33}=-Q_{\zeta}(\iota)$.

Then, by applying Schur complement, we have:

$$\begin{bmatrix} \bar{\Upsilon}_{\zeta}^{11} & \Upsilon_{\zeta}^{12} & 0 & \Upsilon_{\zeta}^{14} & \Upsilon_{\zeta}^{15} \\ * & \Upsilon_{\zeta}^{22} & 0 & \lambda_2\Upsilon_{\zeta}^{14} & \lambda_2\Upsilon_{\zeta}^{15} \\ * & * & \Upsilon_{\zeta}^{33} & 0 & 0 \\ * & * & * & -{\gamma_2}^2 I & 0 \\ * & * & * & * & \Upsilon_{\zeta}^{55} \end{bmatrix}<0, \tag{3.17}$$

where
$\bar{\Upsilon}_{\zeta}^{11} = M_{\zeta}{}^{T}(A_{\zeta h} + B_{\zeta h}) + (A_{\zeta h} + B_{\zeta h})^{T} M_{\zeta} + Q_{\zeta}(\iota) + C_{\zeta}{}^{T} C_{\zeta}, \quad \Upsilon_{\zeta}^{12} = P_{\zeta}(\iota) - M_{\zeta}{}^{T} + \lambda_2 (A_{\zeta h} + B_{\zeta h})^{T} M_{\zeta},$
$\Upsilon_{\zeta}^{22} = -\lambda_2 M_{\zeta}{}^{T} - \lambda_2 M_{\zeta} + \tau_h R_{\zeta}(\iota), \quad \Upsilon_{\zeta}^{14} = M_{\zeta}{}^{T} E_{\zeta}, \quad \Upsilon_{\zeta}^{33} = -Q_{\zeta}(\iota), \Upsilon_{\zeta}^{15} = M_{\zeta}{}^{T} B_{\zeta h}, \quad \Upsilon_{\zeta}^{55} = -\tau_h{}^{-1} R_{\zeta}(\iota).$
$P_{\zeta}(\iota) = \sum_{i=1}^{4} h_i(\iota)(P_{\zeta 0} + P_{\zeta i}), \quad Q_{\zeta}(\iota) = \sum_{i=1}^{4} h_i(\iota)(Q_{\zeta 0} + Q_{\zeta i}), \quad R_{\zeta}(\iota) = \sum_{i=1}^{4} h_i(\iota)(R_{\zeta 0} + R_{\zeta i}).$
M_{ζ} and $\lambda_2 M_{\zeta}$ are slack matrices and $\hat{M}_{\zeta} = M_{\zeta}{}^{-1}$, $\hat{P}_{\zeta}(\iota) = \hat{M}_{\zeta}^{T} P_{\zeta}(\iota) \hat{M}_{\zeta}, \hat{Q}_{\zeta}(\iota) = \hat{M}_{\zeta}^{T} Q_{\zeta}(\iota) \hat{M}_{\zeta}$, $\hat{R}_{\zeta}(\iota) = \hat{M}_{\zeta}^{T} R_{\zeta}(\iota) \hat{M}_{\zeta}$.

The following conditions can be obtained through pre-multiplying and post-multiplying by T_{ζ} and $T_{\zeta}{}^{T}$ to (3.17).

$$\sum_{i=1}^{4} \sum_{j=1}^{4} h_i(\iota) h_j(\iota) \Pi_{ij} < 0, \tag{3.18}$$

where

$$T_{\zeta} = \begin{bmatrix} M_{\zeta}{}^{T-1} & -\frac{1}{\lambda_2} M_{\zeta}{}^{T-1} & 0 & 0 & 0 \\ 0 & M_{\zeta}{}^{T-1} & 0 & 0 & 0 \\ 0 & 0 & M_{\zeta}{}^{T-1} & 0 & 0 \\ 0 & 0 & 0 & I & 0 \\ 0 & 0 & 0 & 0 & M_{\zeta}{}^{T-1} \end{bmatrix}.$$

Based on Lemma 2, inequalities (3.13) are hold. The proof is completed.

4. Simulation results

Table 1. Parameters of vehicle.

Notation	Description	value
m_v	Total mass of vehicle	1530-1680kg
I_z	Yaw moment of inertia	4200-4600$kg \cdot m^2$
l_f	Distance from front axle to CG	1.67m
l_r	Distance from front axle to CG	1.11m
C_f	Front tire cornering stiffness	95000 N/rad
C_r	Rear tire cornering stiffness	85500 N/rad

The parameters of vehicle are given in Table 1. The longitudinal speed of the vehicle v_x is set at 25 m/s. To illustrate the proposed method is superior to the existing CLKF [35] (Corollary 1), the comparison is performed by considering the system (2.13). From Table 2, we can see that the proposed method with $\lambda_1 = 0.1$ has a smaller H_∞ performance index and bigger time delay, that is, the result of path-independent FLKF and introduced slack matrices M_{ϱ} and $\lambda_1 M_{\varrho}$ can obtain less conservative design.

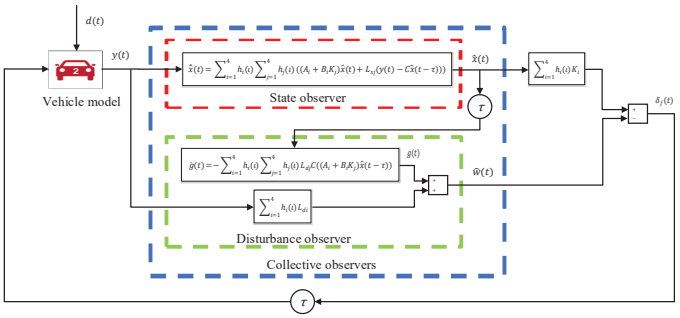

Figure 3. Schematic diagram of simulations for the vehicle AFS.

Table 2. Minimizing the H_∞ performance index and maximizing delay.

Method	γ_1 ($\tau_h = 0.19$)	τ_h ($\gamma_1 = 0.2$)
Theorem 1 (path-independent FLKF (λ_1=0.1))	0.061	0.063
Corollary 1 (CLKF [35](λ_1=0.1))	0.065	0.061
Theorem 1 (path-independent FLKF (λ_1=1))	0.17	0.025

To testify the effectiveness of the proposed control strategy, two cases of simulation are implemented on Matlab /Simulink-Carsim (as shown in Figure 3). In case 1, the persistent side wind force is used as disturbance and different vehicle mass m_v is considered. In case 2, the intermittent side wind force is used as disturbance and different yaw moment of inertia is considered. The D-Class Sedan car is chosen by Carsim to express the vehicle dynamics. The vehicle mass m_v and yaw moment of inertia I_z are $1600kg$ and $4400kg \cdot m^2$, respectively unless specified. The input time delay τ_h is assumed to $0.19\ s$. The parameters λ_1 and λ_2 are both 0.1. By applying Theorem 1 and Theorem 2, the minimum values of γ_1 and γ_2 are 0.061 and 0.37, respectively, and the matrices L_{si}, L_{di} and K_i are given as:

$$L_{s1} = \begin{bmatrix} 49.1209 \\ 31.0100 \end{bmatrix}, \quad L_{s2} = \begin{bmatrix} 54.3644 \\ 30.6819 \end{bmatrix}, \quad L_{s3} = \begin{bmatrix} 38.1701 \\ 30.0822 \end{bmatrix}, \quad L_{s4} = \begin{bmatrix} 48.5045 \\ 31.0602 \end{bmatrix}.$$

$$L_{d1} = 0.9815, \quad L_{d2} = 1.0689, \quad L_{d3} = 0.9848, \quad L_{d4} = 1.0649.$$

$$K_1 = \begin{bmatrix} 0.0345 & -0.7803 \end{bmatrix}, \quad K_2 = \begin{bmatrix} 0.0328 & -0.9304 \end{bmatrix},$$

$$K_3 = \begin{bmatrix} 0.0711 & -0.8966 \end{bmatrix}, \quad K_4 = \begin{bmatrix} 0.0525 & -0.8589 \end{bmatrix}.$$

4.1. Case 1: Persistent side wind force

In the following statements, Figure 4 shows the real persistent side wind force and its estimated value for the system with mass of 1540 kg and 1670 kg, which can be seen that the estimated values are generally consistent with the real values. Figures 5 and 6 show the lateral velocity and yaw rate with mass of 1540 kg, from which we observe that the absolute value of lateral velocity and yaw rate with anti-disturbance controller are 0.0061 m/s and 0.0953 deg/s, and quickly recovered to zero when disturbance is not increased, the absolute value of the lateral velocity and yaw rate controlled by H_∞ method is maintained at 0.0361 m/s and 0.4616 deg/s with the persistent disturbance respectively.

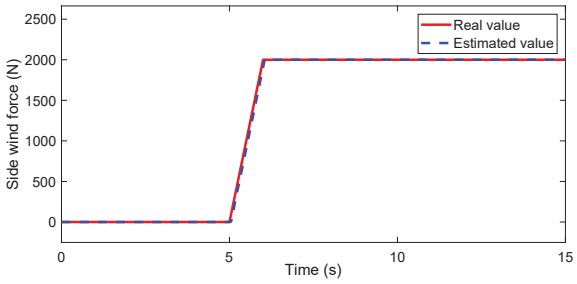

Figure 4. Persistent side wind force.

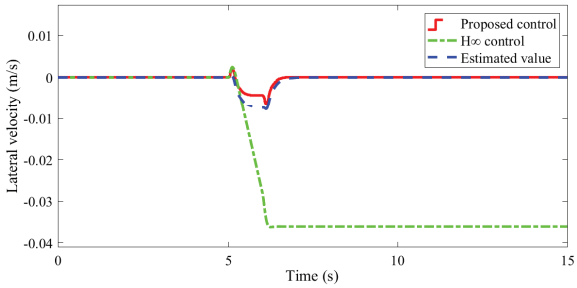

Figure 5. Lateral velocity for Case 1(m = 1540 kg).

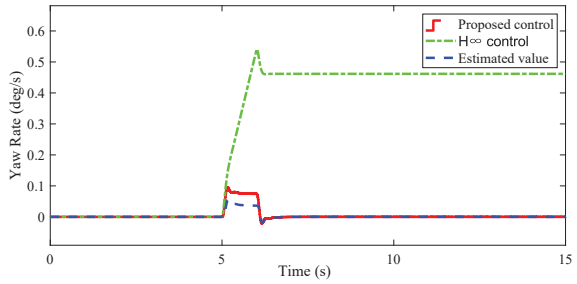

Figure 6. Yaw rate for Case 1(m = 1540 kg).

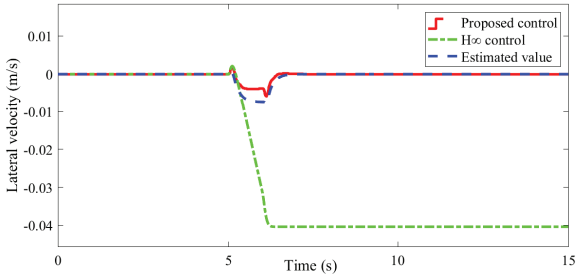

Figure 7. Lateral velocity for Case 1(m = 1670 kg).

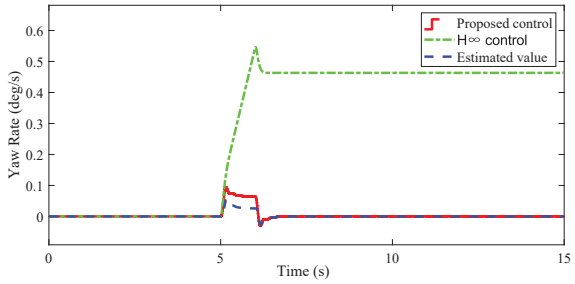

Figure 8. Yaw rate for Case 1($m = 1670\ kg$).

Figures 7 and 8 are the lateral velocity and yaw rates when the mass is 1670 kg. We can observe Figures 7 and 8 that the trend of the lateral velocity and yaw rate are same as Figures 5 and 6, the differences are the maximum absolute value of lateral velocity and yaw rate under anti-disturbance control are 0.0061 m/s and 0.0947 deg/s respectively, and the absolute value of lateral velocity and yaw rate with H_∞ method keep at 0.0404 m/s and 0.4633 deg/s under the persistent disturbance.

4.2. Case 2: Intermittent side wind force

Intermittent side wind force and its observations under two different yaw moment of inertia are given in Figure 9, from which we can be seen that disturbance estimation values can track their real values well. Figures 10 and 11 are lateral velocity and yaw moment of inertia of 4200 $kg \cdot m^2$, respectively. From which we can observe that the absolute maximum lateral velocity and yaw rate under anti-disturbance control are 0.0122 m/s and 0.1973 deg/s. However, the absolute maximum lateral velocity and yaw rate with H_∞ are 0.0855 m/s and 1.154 deg/s, respectively.

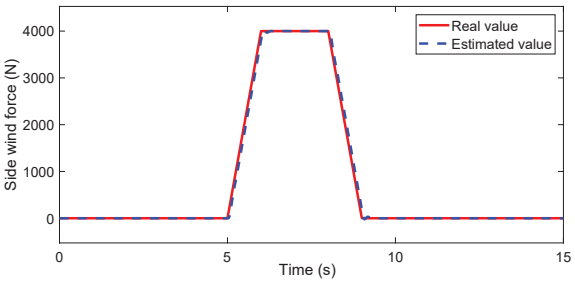

Figure 9. Intermittent side wind force.

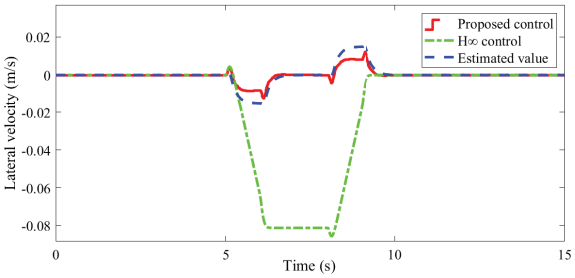

Figure 10. Lateral velocity for Case 2($I_z = 4200\ kg \cdot m^2$).

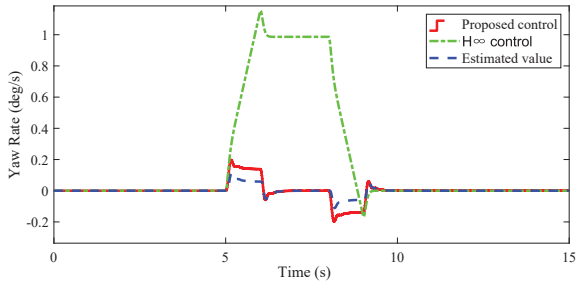

Figure 11. Yaw rate for Case 2($I_z = 4200\ kg \cdot m^2$).

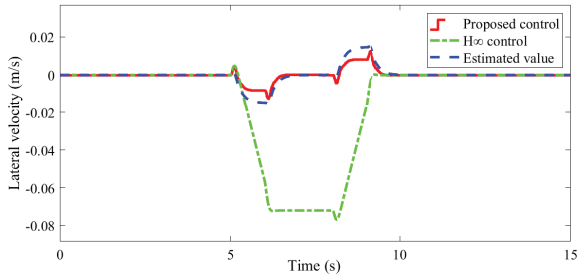

Figure 12. Lateral velocity for Case 2($I_z = 4600\ kg \cdot m^2$).

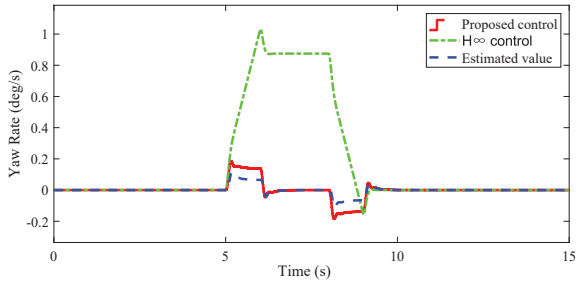

Figure 13. Yaw rate for Case 2($I_z = 4600\ kg \cdot m^2$).

When the inertial moment is selected at 4600 $kg \cdot m^2$, the lateral velocity and yaw rate are shown in Figures 12 and 13, respectively. As seen in Figures 12 and 13, the absolute maximum lateral velocity and yaw rate are 0.0124 m/s and 0.1839 deg/s by anti-disturbance control strategy, respectively. And the absolute maximum lateral velocity and yaw rate with H_∞ control are 0.0768 m/s and 1.032 deg/s, respectively. The estimation of lateral velocity and yaw rate can track real values well.

As shown in above simulation results under two different cases, the proposed collective observers could well estimate the system disturbance and states. It should be pointed out that the smaller the value of the system states, the better the stability of the system. Compared with the H_∞ method, the anti-disturbance control strategy under the strong side wind forces shows better robustness. Furthermore, the system model (1) is established when the tire-ground steering angle is small, which means the lateral velocity must be controlled in a small range. Therefor, the H_∞ control is not suitable for vehicle lateral stability control with strong side wind force.

5. Conclusions

In this paper, new collective observers are proposed to estimate the state and disturbance of vehicle steering system with input time delay. Then the anti-disturbance controller based on collective observers is designed. In stability analysis of collective observers and anti-disturbance controller, a novel path-independent FLKF was constructed to reduce conservatism. The simulation results show that the estimation of system state and disturbance by the proposed collective observers can track its real value very well. It should be pointed out that a small but undesired steering angle can also lead to instability of the vehicle at high speed. And as the disturbance caused by actuator (steering angle) can not be rejected by active anti-disturbance. Our future research will work on a hybrid control method under side wind force and steering angle generated by driver.

Acknowledgments

This research was supported by the China University Industry-University-Research Innovation Fund under Grants 2022BL066, by NSF of Jiangsu Province BK20220444 and NSF Project of Colleges in Jiangsu Province 22KJB120004.

Conflict of interest

We declare that we do not have any commercial or associative interest that represents a conflict of interest in connection with the paper submitted.

References

1. L. Li, D. Wen, N. N. Zhang, L. C. Shen, Cognitive cars: A new frontier for ADAS research, *IEEE Trans. Intell. Transp. Syst.*, **13** (2011), 395–407. http://doi.org/10.1109/TITS.2011.2159493
2. B. Lenzo, M. Zanchetta, A. Sorniotti, P. Gruber, W. D. Nijs, Yaw rate and sideslip angle control through single input single output direct yaw moment control, *IEEE Trans. Control. Syst. Technol.*, **29** (2020), 124–139. http://doi.org/10.1109/TCST.2019.2949539
3. J. Liu, Q. Dai, H. Guo, J. Z. Guo, H. Chen, Human-oriented online driving authority optimization for driver-automation shared steering control, *IEEE Trans. Intell. Veh.*, **7** (2022), 863–872. http://doi.org/10.1109/TIV.2022.3165931
4. H. E. Aiss, K. A. Barbosa, A. A. Peters, Nonlinear Time-Delay Observer-Based Control to Estimate Vehicle States: Lateral Vehicle Model, *IEEE Access*, **10** (2022), 110459–110472. http://doi.org/10.1109/ACCESS.2022.3210566
5. C. A. La, S. D. Gennaro, Nonlinear adaptive tracking for ground vehicles in the presence of lateral wind disturbance and parameter variations, *J. Franklin Inst.*, **354** (2017), 2742–2768. http://doi.org/10.1016/j.jfranklin.2017.01.020
6. Q. Meng, T. Zhao, C. Qian, Z. Sun, P. Ge, Integrated stability control of AFS and DYC for electric vehicle based on non-smooth control, *Int. J. Syst. Sci.*, **10** (2018), 1518–1528. https://doi.org/10.1080/00207721.2018.1460410

7. F. Yakub, Y. Mori, Enhancing path following control performance of autonomous ground vehicle through coordinated approach under disturbance effect, *IEEJ Trans. Electron. Inf. Syst.*, **135** (2015), 102–110. https://doi.org/10.1541/ieejeiss.135.102
8. J. Zhang, H. Wang, M. Ma, M. Yu, A. Yazdani, L. Chen, Active front steering-based electronic stability control for steer-by-wire vehicles via terminal sliding mode and extreme learning machine, *IEEE Trans. Veh. Technol.*, **69** (2020), 14713–14726. https://doi.org/10.1109/TVT.2020.3036400
9. D. Huang, C. Yang, Z. Ju, S. Dai, Disturbance observer enhanced variable gain controller for robot teleoperation with motion capture using wearable armbands, *Auton. Robot.*, **44** (2020), 1217–1231. https://doi.org/10.1007/s10514-020-09928-7
10. N. Huang, J. S. Yang, A. W. Verl, W. Xu, Disturbance observer-based controller for mimicking mandibular motion and studying temporomandibular joint reaction forces by a chewing robot, *2020 IEEE/ASME International Conference on Advanced Intelligent Mechatronics (AIM2020)*, Boston, Massachusetts, USA, 2020, 1042–1047. http://doi.org/10.1109/AIM43001.2020.9158891
11. W. Ren, Q. Qiao, K. Nie, Y. Mao, Robust DOBC for stabilization loop of a two-axes gimbal system, *IEEE Access*, **7** (2019), 110554–110562. https://doi.org/10.1109/ACCESS.2019.2933447
12. W. Bu, T. Li, J. Yang, Y. Yi, Disturbance observer-based event-triggered tracking control of networked robot manipulator, *Meas. Control*, **53** (2020), 892–898. https://doi.org/10.1177/0020294020911084
13. M. A. Abbasi, A. R. Husain, N. R. N. Idris, W. Anjum, H. Bassi, M. J. H. Rawa Predictive flux control for induction motor drives with modified disturbance observer for improved transient response, *IEEE Access*, **8** (2020), 112484–112495. https://doi.org/10.1109/ACCESS.2020.3003005
14. M. V. Nguyen, T. V. Duy, M. C. Ta, Comparative study of disturbance observer-based control and active disturbance rejection control in brushless DC motor drives, *2019 IEEE Vehicle Power and Propulsion Conference (VPPC)*, Hanoi, Vietnam, 2019, 1–6. https://doi.org/10.1109/VPPC46532.2019.8952367
15. B. Xu, Composite learning finite-time control with application to quadrotors, *IEEE Trans. Syst. Man Cybern.: Syst.*, **48** (2017), 1806–1815. https://doi.org/10.1109/TSMC.2017.2698473
16. B. Xu, F. Sun, Composite intelligent learning control of strict-feedback systems with disturbance, *IEEE Trans. Cybern.*, **48** (2017), 730–741. https://doi.org/10.1109/TCYB.2017.2655053
17. J. Xu, X. Sun, J. Qian, Hybrid disturbance observer-based anti-disturbance composite control with applications to mars landing mission, *IEEE Trans. Syst. Man Cybern.: Syst.*, **51** (2019), 2885–2893. https://doi.org/10.1109/TSMC.2019.2917528
18. J. Qiao, Z. Liu, W. Li, Anti-disturbance attitude control of combined spacecraft with enhanced control allocation scheme, *Chin. J. Aeronaut.*, **31** (2018), 1741–1751. https://doi.org/10.1016/j.cja.2018.06.009
19. J. Chen, R. Sun, B. Zhu, Disturbance observer-based control for small nonlinear UAV systems with transient performance constraint, *Aerosp. Sci. Technol.*, **105** (2020), 28–45. https://doi.org/10.1016/j.ast.2020.106028

20. J. Qiao, X. Li, J. Xu, A composite disturbance observer and H_∞ control scheme for flexible spacecraft with measurement delay and input delay, *Chin. J. Aeronaut.*, **32** (2019), 1472–1480. https://doi.org/10.1016/j.cja.2018.10.013

21. T. Feng, Y. Wang, Q. Li, Coordinated control of active front steering and active disturbance rejection sliding mode-based DYC for 4WID-EV, *Meas. Control*, **53** (2020), 1870–1882. https://doi.org/10.1177/0020294020959111

22. J. Feng, Z. Wang, H. Li, W. Zhao, Path following control of autonomous four-wheel-independent-drive electric vehicles via second-order sliding mode and nonlinear disturbance observer techniques, *IEEE Trans. Ind. Electron.*, **68** (2020), 2460–2469. https://doi.org/10.1109/TIE.2020.2973879

23. S. Coskun, L. Li, Vehicle lateral motion control via robust delay-dependent Takagi-Sugeno strategy, *IEEE Trans. Ind. Electron.*, **43** (2021), 1430–1444. https://doi.org/10.1177/0142331220979946

24. L. Zhang, Y. Wang, Z. Wang, Robust lateral motion control for in-wheel-motor-drive electric vehicles with network induced delays, *IEEE Trans. Veh. Technol.*, **68** (2019), 10585–10593. https://doi.org/10.1109/TVT.2019.2942628

25. W. Cao, J. Liu, J. Li, Q. Yang, H. He, Networked motion control for smart EV with multiple-package transmissions and time-varying network-induced delays, *IEEE Trans. Ind. Electron.*, **69** (2021), 4076–4086. https://doi.org/10.1109/TIE.2021.3070499

26. C. Zhang, J. Hu, J. Qiu, W. Yang, H. Sun, Q. Chen, A novel fuzzy observer-based steering control approach for path tracking in autonomous vehicles, *IEEE Trans. Fuzzy Syst.*, **27** (2018), 278–290. https://doi.org/10.1109/TFUZZ.2018.2856187

27. X. Jin, Z. Yu, G. Yin, J. Wang, Improving vehicle handling stability based on combined AFS and DYC system via robust Takagi-Sugeno fuzzy control, *IEEE Trans. Intell. Transp. Syst.*, **19** (2017), 2696–2707. https://doi.org/10.1109/TITS.2017.2754140

28. W. Li, Z. Xie, J. Zhao, J. Gao, Y. Hu, P. K. Wong, Human-Machine Shared Steering Control for Vehicle Lane Keeping Systems via a Fuzzy Observer-Based Event-Triggered Method, *IEEE Trans. Intell. Transp. Syst.*, **23** (2021), 13731–13744. https://doi.org/10.1109/TITS.2021.3126876

29. L. Wang, H. K. Lam, A new approach to stability and stabilization analysis for continuous-time Takagi-Sugeno fuzzy systems with time delay, *IEEE Trans. Intell. Transp. Syst.*, **26** (2017), 2460–2465. https://doi.org/10.1109/TFUZZ.2017.2752723

30. Z. Sheng, C. Lin, B. Chen, Q. Wang, An asymmetric Lyapunov-Krasovskii functional method on stability and stabilization for T-S fuzzy systems with time delay, *IEEE Trans. Fuzzy. Syst.*, **30** (2021), 2135–2140. https://doi.org/10.1109/TFUZZ.2021.3076512

31. G. Li, C. Peng, X. Xie, S. Xie, On stability and stabilization of T-S fuzzy systems with time-varying delays via quadratic fuzzy Lyapunov matrix, *IEEE Trans. Fuzzy. Syst.*, **30** (2021), 3762–3773. https://doi.org/10.1109/TFUZZ.2021.3128062

32. Z. Sheng, L. Wang, C. Lin, B. Chen, A Novel Asymmetric Lyapunov-Krasovskii Functional Method to Stability for TCS Fuzzy Systems with Time-Varying Delay, *Int. J. Fuzzy Syst.*, **24** (2022), 949–956. https://doi.org/10.1007/s40815-021-01176-w

33. Y. Qiu, J. H. Park, C. Hua, X. Wang, Stability Analysis of Time-Varying Delay TS Fuzzy Systems Via Quadratic-Delay-Product Method, *IEEE Trans. Fuzzy. Syst.*, **31** (2022), 129–137. https://doi.org/10.1109/TFUZZ.2022.3182786

34. G. Liu, X. Chang, J. H. Park, M. Hu, Fault Detection Observer Design for Nonlinear Systems via Fuzzy Lyapunov Functions, *IEEE Trans. Syst. Man Cybern.: Syst.*, **52** (2022), 6607–6617. https://doi.org/10.1109/TSMC.2022.3147459

35. X. H. Chang, Y. Liu, Quantized Output Feedback Control of AFS for Electric Vehicles With Transmission Delay and Data Dropouts, *IEEE Trans. Intell. Transp. Syst.*, **23** (2022), 16026–16037. https://doi.org/10.1109/TITS.2022.3147481

36. H. Xu, Y. Zhao, W. Pi, Q. Wang, F. Lin, C. Zhang, Integrated Control of Active Front Wheel Steering and Active Suspension Based on Differential Flatness and Nonlinear Disturbance Observer, *IEEE Trans. Veh. Technol.*, **71** (2022), 4813–4824. https://doi.org/10.1109/TVT.2022.3151252

37. A. T. Nguyen, T. Q. Dinh, T. M. Guerra, J. Pan, TakagiCSugeno fuzzy unknown input observers to estimate nonlinear dynamics of autonomous ground vehicles: Theory and real-time verification, *IEEE/ASME Trans. Mechatron.*, **26** (2021), 1328–1338. https://doi.org/10.1109/TMECH.2020.3049070

38. H. Han, J. Chen, H. R. Karimi, State and disturbance observers-based polynomial fuzzy controller, *Inf. Sci.*, **382** (2017), 38–59. https://doi.org/10.1016/j.ins.2016.12.006

39. S. Hao, T. Liu, B. Zhou, Output feedback anti-disturbance control of input-delayed systems with time-varying uncertainties, *Automatica*, **104** (2019), 8–16. https://doi.org/10.1016/j.automatica.2019.02.047

Supplementary

Programs and s-functions are available at: https://github.com/DrXiaokang/Thesis1.git.